ACS Pharmacology & Translational Science

pubs.acs.org/ptsci

Article

EEG Gamma Band Alterations and REM-like Traits Underpin the Acute Effect of the Atypical Psychedelic Ibogaine in the Rat

Joaquín González, Matias Cavelli, Santiago Castro-Zaballa, Alejandra Mondino, Adriano B. L. Tort, Nicolás Rubido, Ignacio Carrera,* and Pablo Torterolo*

Cite This: *ACS Pharmacol. Transl. Sci.* 2021, 4, 517−525

Read Online

ACCESS | Metrics & More | Article Recommendations | Supporting Information

ABSTRACT: Ibogaine is a psychedelic alkaloid that has attracted large scientific interest because of its antiaddictive properties in observational studies in humans as well as in animal models. Its subjective effect has been described as intense, vivid dream-like experiences occurring while awake; hence, ibogaine is often referred to as an oneirogenic psychedelic. While this unique dream-like profile has been hypothesized to aid the antiaddictive effects, the electrophysiological signatures of this psychedelic state remain unknown. We previously showed in rats that ibogaine promotes a waking state with abnormal motor behavior along with a decrease in NREM and REM sleep. Here, we performed an in-depth analysis of the intracranial electroencephalogram during "ibogaine wakefulness". We found that ibogaine induces gamma oscillations that, despite having larger power than control levels, are less coherent and less complex. Further analysis revealed that this profile of gamma activity compares to that of natural REM sleep. Thus, our results provide novel biological evidence for the association between the psychedelic state and REM sleep, contributing to the understanding of the brain mechanisms associated with the oneirogenic psychedelic effect of ibogaine.

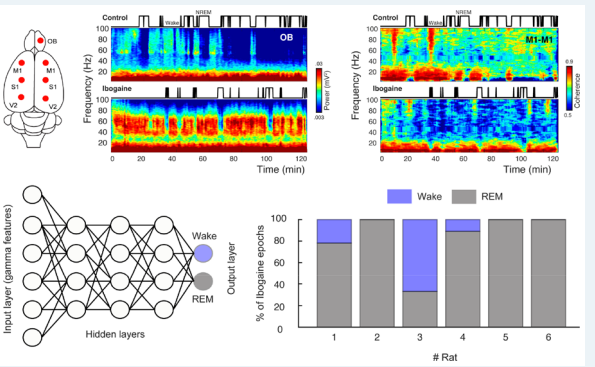

KEYWORDS: *ibogaine, intracranial electroencephalogram, computational neuroscience, sleep-wake cycle, psychedelics*

Ibogaine is a potent psychedelic alkaloid that has attracted scientific interest because of its long-lasting antiaddictive properties,[1] evidenced in anecdotal and observational studies in humans,[2−5] and in extensive preclinical work in rodents.[6−14] Subjective reports portray the ibogaine experience as entering into an intense dream-like episode while awake, involving memory retrieval and prospective imagination, without producing the typical interferences in thinking, identity distortions, and space−time alterations produced by classical psychedelics (e.g., DMT, LSD, psilocybin).[15−18] Thus, ibogaine is often referred to as an oneirogenic psychedelic.[16,18]

In spite of the vast amount of preclinical research regarding the antiaddictive effects of ibogaine, the biological substrate of its unique oneiric effects remains elusive. Although seemingly unrelated, the oneirogenic effects of ibogaine have been hypothesized to aid its antiaddictive properties.[1,19] Taking into account that most vivid dreams occur during REM sleep, the dream-like experiences would be the manifestation of a REM sleep-like brain state, which in turn could favor the antiaddictive effects through an increase in neural plasticity and memory reconsolidation, similar to previously reported functions of natural REM sleep.[20] Therefore, if this conjecture is true, we should expect to find REM sleep characteristics in the electrocortical activity following the administration of ibogaine.

In our previous work,[21] we showed in rats that ibogaine promotes a wakefulness state with abnormal motor behaviors in a dose dependent manner. These effects were accompanied by a decrease in NREM sleep and a profound REM sleep suppression. Nevertheless, as the analysis relied on visual inspection, we were not able to answer which features characterize the waking state induced by ibogaine. Therefore, in the present work we performed a state-of-the-art computational analysis of the intracranial electroencephalogram (iEEG), employing a set of electrodes distributed across the cortex bilaterally, to analyze effects of ibogaine during the first 2 h after its intraperitoneal administration. Upon analyzing the data, we found a unique iEEG profile during wakefulness, which is compatible with a REM-like brain state. Hence, our results provide the first electrophysiological evidence of a wakefulness dream-like brain state produced by ibogaine.

Special Issue: Psychedelics

Received: October 6, 2020
Published: January 11, 2021

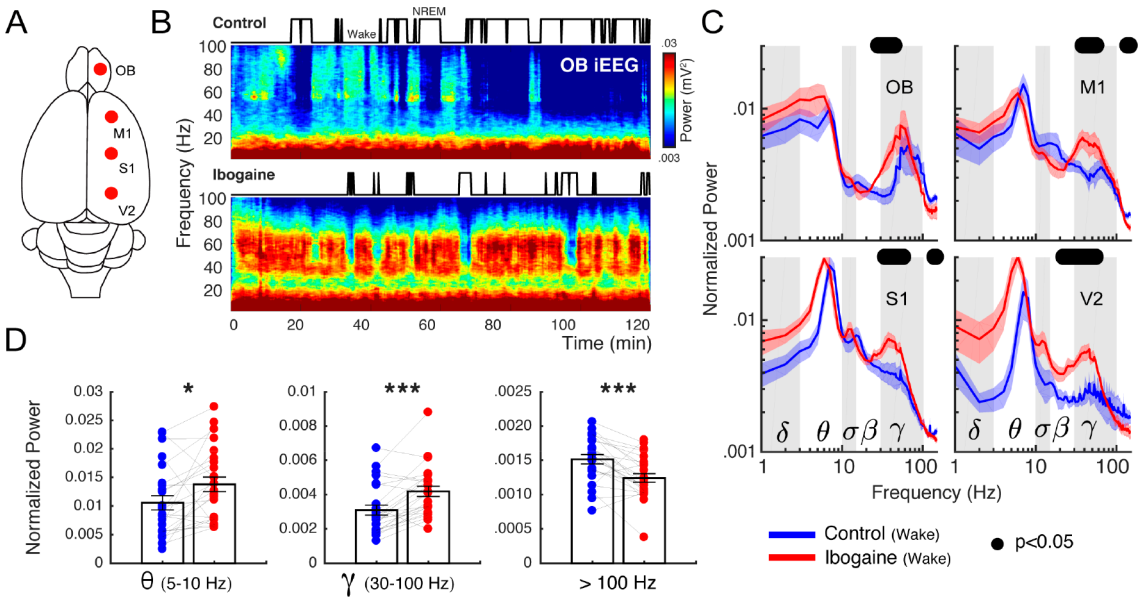

Figure 1. Ibogaine significantly alters iEEG frequency distribution. (A) Location of the analyzed intracranial electrodes in the right hemisphere (OB, olfactory bulb; M1, primary motor cortex; S1, primary somatosensory cortex; V2, secondary visual cortex). (B) Spectrograms from a representative animal following the administration of saline (control) and ibogaine (40 mg/kg). The hypnograms are plotted on top. (C) Normalized power spectra during wakefulness (see Methods for normalization details). The solid line represents the mean (n = 6 animals) for the first 2 h postinjection; the shaded area depicts the standard error of the mean (S.E.M.). The black dots mark the statistically significant frequencies ($p < 0.05$) corrected by a cluster-based permutation test. The traditional frequency bands (Greek letters) are delimited by gray and white boxes in each plot. The differences between hemispheres were minimal (see Figure S2). (D) Mean power for theta, gamma, >100 Hz (up to 512 Hz) frequency bands. Each point corresponds to an electrode of a single animal; bars show mean ± S.E.M. *$p < 0.05$, *** $p < 0.001$, paired t test.

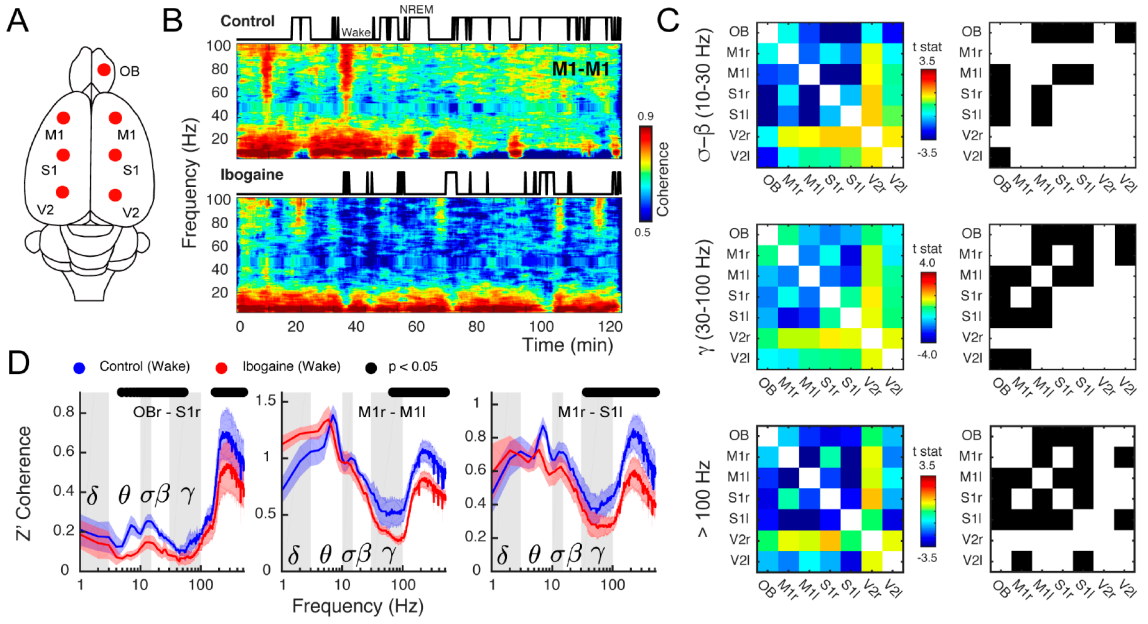

Figure 2. Ibogaine decreases long-range phase synchronization. (A) Location of the analyzed intracranial electrodes. (B) Coherogram following saline (control) and ibogaine (same animal and epoch as in Figure 1B). The hypnograms are plotted on top. This plot shows the phase coherence between the right and left primary motor cortex as a function of time and frequency. (C) The left column shows the t-statistic (t-stat) of the pairwise coherence difference matrix (i.e., the average difference is divided by the S.E.M.) for three frequency bands (sigma-beta, gamma and >100 Hz, up to 512 Hz). The right column shows the electrode pairs with a significant difference ($p < 0.05$, corrected cluster-based permutation test; r, right; l, left). (D) Z′ coherence as a function of frequency of three representative combinations of electrodes (same labels, statistical analysis, and wakefulness epochs as in Figure 1C).

RESULTS

Ibogaine Alters iEEG Oscillatory Components. To understand the acute effects of ibogaine on the rat brain, we recorded iEEG signals following its intraperitoneal administration (40 mg/kg). Electrodes were located above the olfactory bulb (OB), primary motor (M1), primary somatosensory (S1) and secondary visual cortex (V2), allowing us to monitor the dynamical and regional effects of ibogaine (Figure 1A). As a

https://dx.doi.org/10.1021/acsptsci.0c00164
ACS Pharmacol. Transl. Sci. 2021, 4, 517−525

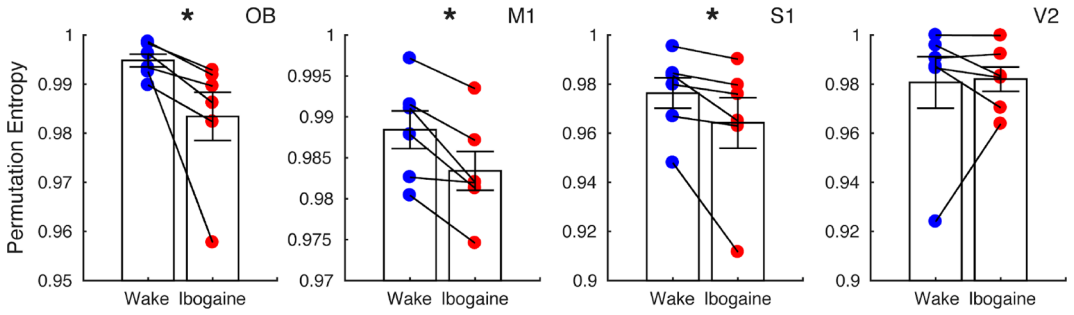

Figure 3. Ibogaine decreases iEEG complexity. Permutation entropy is employed to quantify the iEEG temporal complexity in normal (blue) and ibogaine (red) wake states (same electrodes as in Figure 1). Each dot shows the average permutation entropy of an animal ($n = 6$). Bars represent mean ± S.E.M. *$p < 0.05$, paired t test.

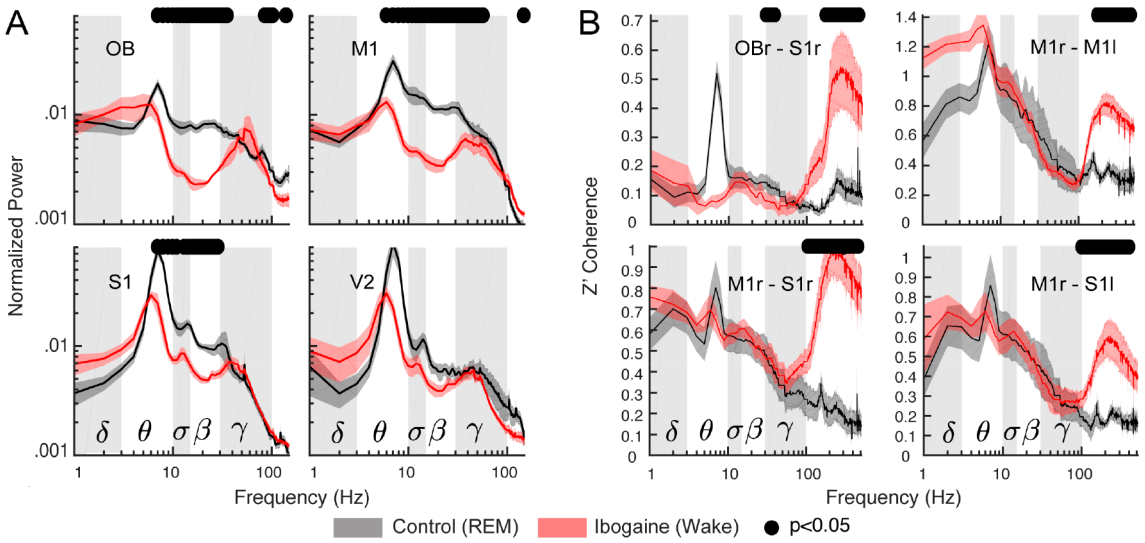

Figure 4. The ibogaine wakefulness shows REM sleep features in the gamma band. (A) Power spectrum comparison between REM sleep (black) and the ibogaine wakefulness (red); only the right hemisphere is shown. The solid line represents the mean ($n = 6$ animals); the shaded area depicts the S.E.M. (B) Coherence comparisons between REM sleep and ibogaine. The black dots mark the statistically significant frequencies ($p < 0.05$) corrected by a cluster-based permutation test.

working example, Figure 1B shows the OB time-frequency response after we administered saline (control) and ibogaine; time zero corresponds to the moment of injection. Compared to control, gamma oscillations (30−80 Hz) increased following the administration of ibogaine; this increase lasted for at least 2 h. Note that this higher gamma power occurred associated with a longer time the animal spent awake (shown in the hypnogram). To analyze ibogaine effects at the group level, we considered only the wakefulness episodes in experimental and control conditions (Figure 1)C. In comparison to control, ibogaine significantly increased gamma oscillations in the OB, M1, S1, and V2 areas (Figure 1C, and summarized in Figure 1D).

Along with the changes in gamma frequencies, the mean theta power increased (Figure 1D), while also decreasing its peak frequency from 9 to 8 Hz (readily observed in S1 and V2 cortices because of their proximity to the hippocampus, Figure S1). Additionally, the high-frequency power (>100 Hz and up to 512 Hz) decreased in M1, S1, and V2 (see Figure 1C,D), though the lack of a spectral peak suggests this result arises from changes in muscular activity produced by the drug.[22]

Ibogaine Decreases Inter-regional Synchronization. Since ibogaine significantly altered the oscillatory power content of the iEEG, we next quantified its impact on long-range synchronization of brain areas within and across hemispheres (Figure 2A). Figure 2B shows an example of interhemispheric coherence between M1 cortices as a function of time (same animal as in Figure 1B). Interestingly, as opposed to its effect on gamma power, ibogaine strongly decreased inter-regional gamma synchronization.

Figure 2C shows a group level analysis separated by frequency bands by means of pairwise electrode matrices (left column), which depict coherence differences (t-statistic) between conditions (saline vs ibogaine) in pseudocolor scale for each electrode pair (blue indicates a coherence decrease while red an increase). The electrode pairs with significant differences are also indicated in the right column. Ibogaine decreased phase coherence at the sigma-beta, gamma, and high-frequency bands in multiple cortical areas, including the OB, M1, and S1 (Figure 2C,D). In particular, inter-regional gamma coherence decreased in 9 of the 21 electrode pairs, including between right OB and right S1 cortex (Figure 2D, left panel), two areas that had an increase in their gamma power (Figure 1C). The same gamma coherence reduction occurred in the interhemispherical M1−M1 and M1−S1 electrode combination, but not in the intrahemispherical M1−S1 (see Figure 2D and Figure S3).

Ibogaine Decreases iEEG Temporal Complexity. In the previous sections, we showed that ibogaine promoted local gamma oscillations which were uncoupled between areas. This

https://dx.doi.org/10.1021/acsptsci.0c00164
ACS Pharmacol. Transl. Sci. 2021, 4, 517−525

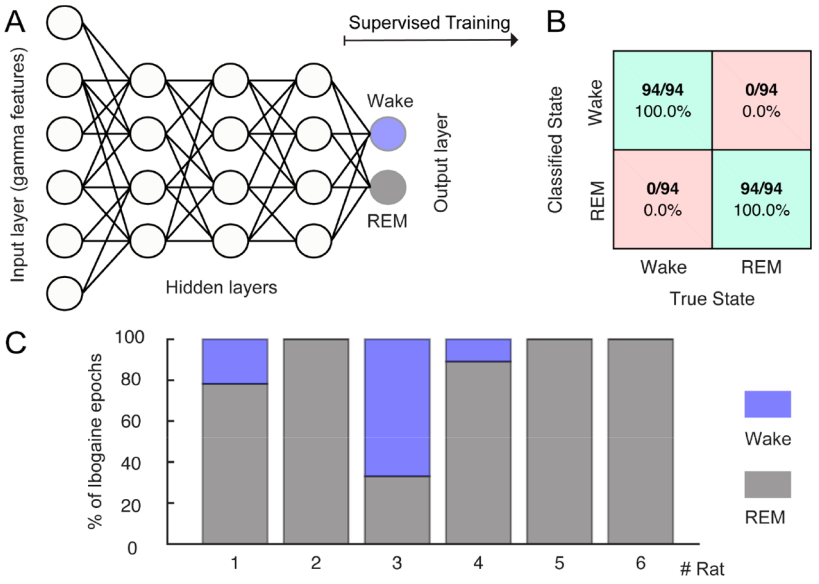

Figure 5. The ibogaine-induced brain state is considered a REM-like state by an automatic sleep scoring algorithm. (A) Schematic representation of the neural network employed to classify the states of wakefulness and REM sleep. The network contains one input layer which receives the gamma features (power and coherence of the OB, M1, and S1 electrodes), and 10 hidden layers (only three of them are shown in the picture). The network has one output layer with two nodes (wake and REM). (B) Confusion matrix for an individual animal. (C) Bar plots showing how ibogaine wakefulness epochs were classified. Each animal is shown separately and was tested with its own control network.

activity resembles gamma oscillations that naturally occur during REM sleep[23−25] (Figure S4), suggesting that the awake state under ibogaine exhibits similar REM sleep characteristics. To delve further into this matter, we tested the resemblance between states in their temporal complexity. This is important because the temporal complexity during REM sleep is significantly lower than during wakefulness, which can be observed independent of the cortical area and for a wide range of time-scales.[26]

To assess the temporal complexity, we down-sampled the original signals to 128 Hz (avoiding muscular contamination) and measured the permutation entropy of the time-series. This metric quantifies the diversity of dynamical motifs in the iEEG (larger values mean the signal has higher diversity, hence more complexity) and is robust to the presence of noise and short time measurements (see Material and Methods and.[27] Figure 3 shows the average permutation entropy for each cortical electrode. Interestingly, in comparison to normal (control) wakefulness, ibogaine wakefulness displayed significantly lower levels of dynamical complexity in OB, M1 and S1 cortex. Note that these areas are the ones with most prominent changes in power and coherence. No significant changes were observed in V2. We should also point out that by virtue of downsampling, the gamma band oscillations are the only relevant frequencies contained in our complexity estimate.

Ibogaine Wakefulness and REM Sleep Have Similar iEEG Gamma Activity. The previous section showed that the ibogaine awake state differs from normal wakefulness. We next compared the ibogaine-induced brain state with physiological REM sleep (Figure 4A). We found that theta, sigma, and beta power were lower during ibogaine wakefulness than in REM sleep. On the other hand, the high-frequency component (>100 Hz) had significantly higher power, likely due to muscular activity. Noteworthy, the power of gamma oscillations was similar between both states and minor statistically significant differences were found in the OB and M1 with larger gamma power during REM (Figure 4A). Furthermore, we also found similar levels of gamma coherence in the ibogaine wakefulness and REM sleep, even for electrode combinations which showed significant changes between physiological and ibogaine wakefulness (compare Figure 2B with Figure 4C). In contrast, the high-frequency spectrum was more coherent during ibogaine wakefulness than during REM sleep, probably as a consequence of the absence of muscle activity during REM sleep.

We also found that the temporal complexity during the ibogaine wakefulness was close to that of REM sleep (Figure S5); it was only significantly larger during ibogaine wakefulness in the M1 cortex. Overall, the data show that iEEG complexity during ibogaine wakefulness is between normal wakefulness and REM sleep. Thus, although there are differences between ibogaine wakefulness and REM sleep, the power, complexity, and inter-regional synchronization of gamma oscillations are comparable.

Finally, we directly tested whether the ibogaine wakefulness was closer to a REM-like state or to physiological wakefulness. For this purpose, we trained an artificial neural network to automatically classify the states of wakefulness and REM sleep. Figure 5A shows a schematic representation of the network, which is fed with the levels of gamma power, and coherence of single 10-s artifact free epochs (input layer) and the output were the behavioral states (wake or REM, output layer). After supervised training, the network successfully distinguished between wakefulness and REM (the confusion matrix for a representative animal is shown in Figure 5B). Then, the network was fed with ibogaine wakefulness data, these epochs were mostly classified as being REM sleep instead of wakefulness (Figure 5C). In fact, in 5 out of 6 animals the majority of the ibogaine epochs were classified as REM sleep, and in 3 animals all ibogaine epochs were classified as such. Therefore, these results show that the gamma oscillations induced by ibogaine have convincing REM sleep-like features.

https://dx.doi.org/10.1021/acsptsci.0c00164
ACS Pharmacol. Transl. Sci. 2021, 4, 517−525

DISCUSSION

In the present study, we found that intraperitoneal administration of ibogaine in male rats induces a waking brain state that has electrocortical REM sleep traits. These traits appear in the form of high-power local gamma oscillations in the OB, M1, S1 areas, which are less coherent and less complex than in normal wakefulness. These features of gamma oscillations are similar to the ones present during REM sleep (Figures 4 and 5 and Figure S4). Therefore, by measuring an important neurophysiological trait, our results support previous oneirogenic conjectures of ibogaine's induced psychedelic state.[1,19] Interestingly, some of these traits were dragged into NREM sleep; compared to physiological NREM sleep, ibogaine NREM sleep showed gamma power increase circumscribed to the OB, and lower gamma coherence in several derivations (Figure S6). It should be noted, however, that our results only suggest the oneirogenic nature of the ibogaine state, but do not provide further evidence of the relationship between this oneiric state and the antiaddictive properties of ibogaine.

The relationship between this unique wakefulness promoted by ibogaine and the antiaddictive properties is speculative, as another experimental design should be employed to address this matter. However, considering that it had been reported by several ibogaine users that the dream-like experiences helped them change their addictive behaviors, and our findings showing that ibogaine induces a wakefulness state showing REM-like traits (i.e., a dissociate state), it is likely that this unique wakefulness state could be related to its antiaddictive properties. Nevertheless, we cannot rule out that the suppression of REM sleep by itself, could be also related to the antiaddictive effect induced by ibogaine.

When comparing our results to the effects elicited by other psychedelics, the lack of previous reports involving quantitative iEEG analysis of the psychedelic state in rodents forces us to compare our results to previous literature in human beings. For instance, the administration of 5-HT_{2A} agonist (e.g., LSD, psilocybin, DMT) in humans reduces alpha (8−12 Hz) and beta band power and decreases their functional connectivity.[28−32] Similarly, our results show that ibogaine also reduced the connectivity at sigma and beta bands (10−30 Hz). Additionally, it is worth noting that we found significant changes in the OB, while in humans the predominant effects of traditional psychedelics are observed in the visual cortex.[29] Thus, both psychedelic effects involve major sensory areas relevant to each species. Furthermore, complementary analyses show that the gamma coupling to other frequencies is not affected by ibogaine in any of the cortical locations (Figure S7). As the slow OB oscillations (1−4 Hz) reflect the slow respiratory potentials,[33,34] our results suggest that sensory information is still likely to reach the OB, but is later integrated in an altered way, similar to the psychedelic state in humans.[28]

In addition to the electrophysiological similarities between ibogaine and serotoninergic psychedelics, the type of cognition elicited by the latter has been described as analogous to the one present during dreams[28] (both referred as primary states of consciousness). In fact, a recent work shows that unlike other drugs (cocaine, opioids, etc.), the semantic content of psychedelic experiences is closely related to dreams.[35] Since dreams are to a large extent the cognitive correlates of REM sleep,[36] our report confirms such connection for ibogaine.

Nevertheless, as mentioned before, human subjective reports also indicate differences between the experience elicited by ibogaine and classic psychedelics. Pharmacological and behavioral data in rodents also support these differences. While classical psychedelics share the ability to interact with the 5-HT_{2A} receptor in the low nanomolar range inducing the head twitch response (HTR) in rodents,[17] ibogaine binds to this receptor in the micromolar range[37,38] without producing HTR or similar responses.[21] Also, previous drug discrimination studies in rats showed that although ibogaine may produce some of its effect via 5-HT_{2A} activation, this does not appear to be essential to the ibogaine-discriminative stimulus, since pirenperone (5-HT_{2A} antagonist) did not affect the ibogaine-appropriate response.[38,39] Further studies employing the same iEEG methodology should shed light into the electrophysiological similarities and differences between the wakefulness state induced by classical psychedelics and ibogaine.

It should be noted that ibogaine is rapidly metabolized (half-life: 1.22 hs) to produce noribogaine, which has its own pharmacological and pharmacokinetic profiles.[40,41] According to pharmacokinetic data,[42] both substances are present in the rat brain at pharmacologically relevant concentrations during the first 2 h after ibogaine 40 mg/kg i.p. administration. Non-competitive antagonism of *N*-methyl-D-aspartate receptors (NMDA-R) by ibogaine[43−48] and to a lesser extent by noribogaine[44,45] should be considered as a key factor to explain the effects on the gamma band, since ketamine (a non-competitive NMDA-R antagonist) also produces a marked increase in gamma power[49−52] while decreasing inter-regional gamma coherence.[51,52]

Nevertheless, effects on other neurotransmitter systems and receptors should be also considered. Since ibogaine and noribogaine inhibit serotonin reuptake by modulating SERT activity (noribogaine being approximately ten-times more potent than ibogaine),[53,54] the increase in serotoninergic transmission, in addition to the above-mentioned interaction of ibogaine with 5HT_{2A} receptor, could explain some of the similarities found in the electrocortical activity between ibogaine and classic psychedelics. Additionally, the potential contribution of the kappa opioid action of noribogaine[55] as a biased agonist should also be considered, as other kappa agonists induce oscillations in the theta range (4−10 Hz),[56−58] resembling our results.

As a final remark, our results show that ibogaine promotes a waking brain state with REM sleep traits. Because most dreams occur during REM sleep, this new finding accounts for the oneirogenic psychedelic effect experienced after ibogaine consumption, thus providing novel biological evidence linking psychedelics and REM sleep.

METHODS

Ibogaine. Ibogaine was obtained and purified from *T. Iboga* extracts following the procedures employed in ref 21 (see Ibogaine Supplementary Information in the Supporting Material for the purification protocol, structure elucidation, and purity profile). A 40 mg/kg dose (i.p.) was employed in this work, which is the effective dose used in the preclinical literature to obtain long lasting effects in the self-administration paradigms in rats, and that in our previous study showed to have the largest effect on the wakefulness−sleep architecture.[21] Dissolution of ibogaine−HCl to prepare the samples for intraperitoneal (i.p.) injection was carried out using warm saline that was previously degassed by nitrogen bubbling (~17 mg of ibo-HCl/mL of saline).

https://dx.doi.org/10.1021/acsptsci.0c00164
ACS Pharmacol. Transl. Sci. 2021, 4, 517−525

Experimental Animals. Six Wistar male adult rats were maintained on a 12-h light/dark cycle (lights on at 07.00 h).

Although to analyze only one gender is a limitation of the study, we took it as a first approach to explore the effects of ibogaine on electrocortical activity. Food and water were freely available. The animals were determined to be in good health by veterinarians of the institution. All experimental procedures were conducted in agreement with the National Animal Care Law (No. 18611) and with the "Guide to the Care and Use of Laboratory Animals" (8th edition, National Academy Press, Washington, DC. 2010). Furthermore, the Institutional Animal Care Committee approved the experimental procedures (Exp. No. 070153-000332-16). Adequate measures were taken to minimize pain, discomfort, or stress of the animals, and all efforts were made to use the minimal number of animals necessary to obtain reliable scientific data. Each animal received the ibogaine and the vehicle dose in different days, and was therefore its own control.

Surgical Procedures. The animals were chronically implanted with electrodes to monitor the states of sleep and wakefulness. We employed similar surgical procedures as in our previous studies.[21,24,25] Anesthesia was induced with a mixture of ketamine−xylazine (90 mg/kg; 5 mg/kg i.p., respectively). The rat was positioned in a stereotaxic frame and the skull was exposed. To record the iEEG, stainless steel screw electrodes were placed in the skull above motor, somatosensory, visual cortices (bilateral), the right olfactory bulb, and cerebellum, which was the reference electrode (see Table S1). To record the electromyogram (EMG), two electrodes were inserted into the neck muscle. The electrodes were soldered into a 12-pin socket and fixed onto the skull with acrylic cement. At the end of the surgical procedures, an analgesic (ketoprofen, 1 mg/kg, s.c.) was administered. After the animals had recovered from these surgical procedures, they were left to adapt in the recording chamber for 1 week.

Experimental Sessions. Animals were housed individually in transparent cages (40 × 30 × 20 cm^3) containing wood shaving material in a temperature-controlled room (21−24 °C), with water and food *ad libitum*. Experimental sessions were conducted during the light period, between 10 AM and 4 PM during the light phase in a sound-attenuated chamber with Faraday shield. Before the beginning of the recordings, animals were injected with a 40 mg/kg ibogaine dose or vehicle i.p. The recordings were performed through a rotating connector, to allow the rats to move freely within the recording box. Polysomnographic data were acquired and stored in a computer using the Dasy Lab Software employing 1024 Hz as a sampling frequency and a 16 bits AD converter.

Sleep Scoring. The states of sleep and wakefulness were determined in 10-s epochs. Wakefulness was defined as low-voltage fast waves in the motor cortex, a noticeable theta rhythm (4−7 Hz) in the somatosensory and visual cortices, and relatively high EMG activity. NREM sleep was determined by the presence of high-voltage slow cortical waves together with sleep spindles in frontal, parietal, and occipital cortices associated with a reduced EMG amplitude; REM sleep as low-voltage fast frontal waves, a regular theta rhythm in the occipital cortex, and a silent EMG except for occasional twitches. Artifacts and transitional epochs were removed employing visual supervision.

Data Analysis. To evaluate the ibogaine effect on iEEG activity, we selected the first 2 h following its i.p. administration (10 AM to 12 AM) since almost continuous wakefulness and abnormal motor and autonomic effects (tremor, piloerection) were only evident during this period.[21] From the first 2 h, only artifact-free wake epochs were analyzed from both the control and ibogaine experiments. NREM sleep epochs were selected from the entire 6 h due to the reduced time of this state after ibogaine i.p. administration. Additionally, REM sleep epochs from control experiments were also examined. REM sleep following ibogaine administration was not considered due to the lack of this state in several animals.

Power Spectrum. The power spectrum was obtained by means of the *pwelch* built-in function in Matlab (parameters: window = 1024, noverlap = [], fs = 1024, nfft = 1024), which corresponds to 1-s sliding windows with half-window overlap, and a frequency resolution of 1 Hz. The time-frequency spectrograms were obtained employing the function *mtspecgramc* from the Chronux toolbox[59] (available at: http://chronux.org), using five tapers and a time-bandwidth product of 5. All spectra were whitened by multiplying the power at each frequency by the frequency itself, thus counteracting the 1/f trend. In addition, the spectra were normalized to obtain the relative power by dividing the power value of each frequency by the sum across frequencies. The traditional frequency bands depicted in the figures were taken as delta (1−4 Hz), theta (5−10 Hz), sigma (11−14 Hz), beta (15−29 Hz), and gamma (30−100 Hz).

Spectral Coherence. To measure synchronization between electrodes, we employed the magnitude squared coherence using the *mscohere* built-in function in Matlab (parameters: window = 1024, noverlap = [], fs = 1024, nfft = 1024), which corresponds to 1-s sliding windows with half-window overlap, and a frequency resolution of 1 Hz. The time-frequency coherograms were obtained employing the function *cohgramc* from the Chronux toolbox, using 10 tapers and a time-bandwidth product of 100.

Cluster-Based Permutation Test. To obtain statistical thresholds for group comparisons of power and coherence, we employed a data-driven approach comparing empirical clusters of frequencies instead of comparing traditionally defined frequency bands. The method consisted of first comparing individual frequencies (512 frequencies) in each condition by means of paired *t* tests ($\alpha = 0.05$). Once we obtained the *p* values for each frequency, all consecutive significant frequencies were grouped into empirical clusters (defining a minimum cluster size of four frequency points), and a new statistic was formed by summing the *t*-statistic of each frequency inside the cluster. To assess whether a given cluster was significant, a null hypothesis distribution of cluster statistics was constructed by randomizing labels (control and ibogaine) and repeating the cluster construction method for a total of 10 000 randomizations. The *p* values of the empirical clusters were obtained by comparing each cluster statistic to the randomized cluster statistic distribution (X). We employed two-tailed comparisons for the power spectrum and permutation entropy ($p_{value} = 2\min(P(X > X_{obs})), P(X < X_{obs}))$, and one-tailed for the coherence comparisons ($p_{value} = P(X < X_{obs})$).

Permutation Entropy. Prior to quantifying the permutation entropy, the iEEGs were down-sampled to 128 Hz. The framework consisted of 2 main steps. In the first step, we encoded the time-series into ordinal patterns (OP) following the Bandt and Pompe method.[27] The encoding involves dividing a time-series $\{x(t), t = 1, \cdots, T\}$ into $\lfloor (T - D)/D \rfloor$ nonoverlapping vectors, where $\lfloor y \rfloor$ denotes the largest integer less than or equal to y and D is the vector length, which is much shorter than the

https://dx.doi.org/10.1021/acsptsci.0c00164
ACS Pharmacol. Transl. Sci. 2021, 4, 517−525

time-series length ($D \ll T$). Then, each vector is classified according to the relative magnitude of its D elements. Namely, we determined how many permutations between neighbors are needed to sort its elements in increasing order; then, an OP represents the vector permutations. The second step consists in applying the Shannon entropy to quantify the average randomness (information content) of the OP distribution. Shannon entropy is defined as $H = -\sum p(\mathrm{OP}) \log[p(\mathrm{OP})]$, where $p(\mathrm{OP})$ is the probability of finding a given OP in the signal (among the set of all OPs), and the summation is carried over all possible OPs. To assess the statistical significance between conditions, we employed paired two-tailed t tests with $\alpha = 0.05$.

Gamma-Band Sleep Scoring Neural Network. A multilayer perceptron (10 hidden layers) was employed to distinguish between the states of wakefulness and REM sleep.

We used the built-in classification network *patternnet* in Matlab. The input to the network consists of values of gamma power (OB, M1r, M1l, S1r) and coherence (the nine significant pairs in Figure 2C). The network was trained through a supervised scheme employing the visually scored states in the control condition (either Wake or REM). The training was performed employing the scaled conjugate gradient backpropagation algorithm (*trainscg* built-in function in Matlab), and the performance of the network was evaluated by the cross-entropy algorithm (*crossentropy* built-in function in Matlab).

Phase-Amplitude Coupling. To measure coupling between frequencies within a same region, we employed the modulation index method.[60] Briefly, the raw signal was filtered between 1 and 15 Hz in 1-Hz steps and 3-Hz bandwidth (*eegfilt* function in EEGLAB;[61] to obtain the slow frequency components, and then the phase time series were extracted from their analytical representation based on the Hilbert transform (*hilbert* built-in function in Matlab). In addition, the same raw signal was also filtered between 40 and 180 Hz in 10 Hz steps (bandwidth 10 Hz) to obtain the faster frequency components, and their amplitude time series are also obtained from the analytical representation. Then, phase-amplitude distributions were computed between all slow-fast frequency combinations. Finally, the modulation index was obtained as $\mathrm{MI} = (H_{\max} - H)/H_{\max}$, where $H_{\max}$ is the maximum possible Shannon entropy for a given distribution (log(number of bins)) and H is the actual entropy. The MI value of each slow-fast frequency combination was plotted in pseudocolor scale to obtain the comodulation maps. To assess the statistical significance between conditions, we employed paired two-tailed t tests with $\alpha = 0.05$.

■ ASSOCIATED CONTENT

Supporting Information

The Supporting Information is available free of charge at https://pubs.acs.org/doi/10.1021/acsptsci.0c00164.

> Electrode location; ibogaine's effect on theta oscillations; ibogaine's effect on right and left hemispheres; coherence between all electrodes; power and coherence during wakefulness and REM sleep; permutation entropy during REM; ibogaine's effects on NREM sleep; ibogaine's effect on cross-frequency coupling; ibogaine chemical supplemental information (PDF)

■ AUTHOR INFORMATION

Corresponding Authors

Pablo Torterolo − *Departamento de Fisiología, Facultad de Medicina, Universidad de la República, Montevideo 11200, Uruguay*; Email: ptortero@fmed.edu.uy

Ignacio Carrera − *Departamento de Química Orgánica, Facultad de Química, Universidad de la República, Montevideo, Uruguay*; orcid.org/0000-0002-6053-3162; Email: icarrera@fq.edu.uy

Authors

Joaquín González − *Departamento de Fisiología, Facultad de Medicina, Universidad de la República, Montevideo 11200, Uruguay*; orcid.org/0000-0002-8721-4292

Matias Cavelli − *Departamento de Fisiología, Facultad de Medicina, Universidad de la República, Montevideo 11200, Uruguay; Department of Psychiatry, University of Wisconsin, Madison, Wisconsin 53558, United States*

Santiago Castro-Zaballa − *Departamento de Fisiología, Facultad de Medicina, Universidad de la República, Montevideo 11200, Uruguay*

Alejandra Mondino − *Departamento de Fisiología, Facultad de Medicina, Universidad de la República, Montevideo 11200, Uruguay; Department of Anesthesiology, University of Michigan, Ann Arbor, Michigan 48103, United States*

Adriano B. L. Tort − *Brain Institute, Federal University of Rio Grande do Norte, Natal, Rio Grande do Norte 59056, Brazil*

Nicolás Rubido − *Aberdeen Biomedical Imaging Centre, University of Aberdeen, Aberdeen AB25 2ZG, United Kingdom; Instituto de Física de Facultad de Ciencias, Universidad de la República, Montevideo 11400, Uruguay*

Complete contact information is available at: https://pubs.acs.org/10.1021/acsptsci.0c00164

Author Contributions

J.G., M.C., I.C., and P.T. designed the experiments; J.G., M.C., and A.M., conducted the experiments; J.G. and N.R., wrote analysis software; J.G. analyzed the data; J.G., M.C., A.M., S.C., N.R., A.B.L.T., I.C., and P.T. were involved in the discussion and interpretation of the results; J.G., A.B.L.T., I.C., and P.T. wrote the manuscript. All the authors participated in the critical revision of the manuscript, added important intellectual content, and approved the final version.

Notes

The authors declare no competing financial interest.

Data and code availability. Data is available under request to the authors. The codes to obtain power and coherence spectra can be found in the Chronux toolbox and standard Matlab toolboxes. The code to perform the correction for multiple comparisons based on cluster-based permutation tests and to compute permutation entropy is freely available at https://github.com/joaqgonzar/Ibogaine_analysis_2020. In addition, the specific code employed in the multilayer perceptron is also available upon request.

■ ACKNOWLEDGMENTS

This study was supported by the Programa de Desarrollo de Ciencias Básicas, PEDECIBA; Agencia Nacional de Investigación e Innovación (ANII), (FCE-1-2017-1-136550) and the Comisión Sectorial de Investigación Científica (CSIC) I+D-2016-589 grant from Uruguay. J.G. was supported by CAP (Comisión Académica de Posgrado) and CSIC Iniciación. N.R.

acknowledges the CSIC group Grant CSIC2018-FID 13-Grupo ID 722. A.B.L.T. was supported by Conselho Nacional de Desenvolvimento Científico e Tecnológico (CNPq) and Coordenacao de Aperfeicoamento de Pessoal de Nível Superior (CAPES), Brazil.

REFERENCES

(1) Alper, K. R. (2001) Ibogaine: A Review. *Alkaloids Chem. Biol. 56*, 1−38.
(2) Brown, T. K., and Alper, K. (2018) Treatment of Opioid Use Disorder with Ibogaine: Detoxification and Drug Use Outcomes. *Am. J. Drug Alcohol Abuse 44* (1), 24−36.
(3) Mash, D. C., Duque, L., Page, B., and Allen-Ferdinand, K. (2018) Ibogaine Detoxification Transitions Opioid and Cocaine Abusers Between Dependence and Abstinence: Clinical Observations and Treatment Outcomes. *Front. Pharmacol. 9*, 529.
(4) Noller, G. E., Frampton, C. M., and Yazar-Klosinski, B. (2018) Ibogaine Treatment Outcomes for Opioid Dependence from a Twelve-Month Follow-up Observational Study. *Am. J. Drug Alcohol Abuse 44* (1), 37−46.
(5) Schenberg, E. E., de Castro Comis, M. A., Chaves, B. R., and da Silveira, D. X. (2014) Treating Drug Dependence with the Aid of Ibogaine: A Retrospective Study. *J. Psychopharmacol. 28* (11), 993−1000.
(6) Dzoljic, E. D., Kaplan, C. D., and Dzoljic, M. R. (1988) Effect of Ibogaine on Naloxone-Precipitated Withdrawal Syndrome in Chronic Morphine-Dependent Rats. *Arch. Int. Pharmacodyn. Ther. 294*, 64−70.
(7) Glick, S. D., Rossman, K., Steindorf, S., Maisonneuve, I. M., and Carlson, J. N. (1991) Effects and Aftereffects of Ibogaine on Morphine Self-Administration in Rats. *Eur. J. Pharmacol. 195* (3), 341−345.
(8) Glick, S. D., Rossman, K., Rao, N. C., Maisonneuve, I. M., and Carlson, J. N. (1992) Effects of Ibogaine on Acute Signs of Morphine Withdrawal in Rats: Independence from Tremor. *Neuropharmacology 31* (5), 497−500.
(9) Cappendijk, S. L., and Dzoljic, M. R. (1993) Inhibitory Effects of Ibogaine on Cocaine Self-Administration in Rats. *Eur. J. Pharmacol. 241* (2−3), 261−265.
(10) Glick, S. D., Kuehne, M. E., Raucci, J., Wilson, T. E., Larson, D., Keller, R. W., and Carlson, J. N. (1994) Effects of Iboga Alkaloids on Morphine and Cocaine Self-Administration in Rats: Relationship to Tremorigenic Effects and to Effects on Dopamine Release in Nucleus Accumbens and Striatum. *Brain Res. 657* (1−2), 14−22.
(11) Dworkin, S. I., Gleeson, S., Meloni, D., Koves, T. R., and Martin, T. J. (1995) Effects of Ibogaine on Responding Maintained by Food, Cocaine and Heroin Reinforcement in Rats. *Psychopharmacology (Berl.) 117* (3), 257−261.
(12) Rezvani, A. H., Overstreet, D. H., and Leef, Y. W. (1995) Attenuation of Alcohol Intake by Ibogaine in Three Strains of Alcohol-Preferring Rats. *Pharmacol., Biochem. Behav. 52* (3), 615−620.
(13) Pearl, S. M., Hough, L. B., Boyd, D. L., and Glick, S. D. (1997) Sex Differences in Ibogaine Antagonism of Morphine-Induced Locomotor Activity and in Ibogaine Brain Levels and Metabolism. *Pharmacol., Biochem. Behav. 57* (4), 809−815.
(14) He, D.-Y., McGough, N. N. H., Ravindranathan, A., Jeanblanc, J., Logrip, M. L., Phamluong, K., Janak, P. H., and Ron, D. (2005) Glial Cell Line-Derived Neurotrophic Factor Mediates the Desirable Actions of the Anti-Addiction Drug Ibogaine against Alcohol Consumption. *J. Neurosci. 25* (3), 619−628.
(15) Brown, T. K., Noller, G. E., and Denenberg, J. O. (2019) Ibogaine and Subjective Experience: Transformative States and Psychopharmacotherapy in the Treatment of Opioid Use Disorder. *J. Psychoact. Drugs 51* (2), 155−165.
(16) Naranjo, C. (1974) *The Healing Journey: New Approaches to Consciousness*, Pantheon Books, New York.
(17) Nichols, D. E. (2016) Psychedelics. *Pharmacol. Rev. 68* (2), 264−355.
(18) Schenberg, E. E., de Comis, M. A. C., Alexandre, J. F. M., Tófoli, L. F., Chaves, B. D. R., and da Silveira, D. X. (2017) A Phenomenological Analysis of the Subjective Experience Elicited by Ibogaine in the Context of a Drug Dependence Treatment. *J. Psychedelic Stud. 1* (2), 74−83.
(19) Goutarel, R., Gollnhofer, O., and Salinas, R. (1993) Pharmacodynamics and Therapeutic Applications of Iboga and Ibogaine. *Psychedelic Monogr. Essays 6*, 70.
(20) Izawa, S., Chowdhury, S., Miyazaki, T., Mukai, Y., Ono, D., Inoue, R., Ohmura, Y., Mizoguchi, H., Kimura, K., Yoshioka, M., Terao, A., Kilduff, T. S., and Yamanaka, A. (2019) REM Sleep-Active MCH Neurons Are Involved in Forgetting Hippocampus-Dependent Memories. *Science 365* (6459), 1308−1313.
(21) González, J., Prieto, J. P., Rodríguez, P., Cavelli, M., Benedetto, L., Mondino, A., Pazos, M., Seoane, G., Carrera, I., Scorza, C., and Torterolo, P. (2018) Ibogaine Acute Administration in Rats Promotes Wakefulness, Long-Lasting REM Sleep Suppression, and a Distinctive Motor Profile. *Front. Pharmacol. 9*, 374.
(22) Whitham, E. M., Pope, K. J., Fitzgibbon, S. P., Lewis, T., Clark, C. R., Loveless, S., Broberg, M., Wallace, A., DeLosAngeles, D., Lillie, P., Hardy, A., Fronsko, R., Pulbrook, A., and Willoughby, J. O. (2007) Scalp Electrical Recording during Paralysis: Quantitative Evidence That EEG Frequencies above 20 Hz Are Contaminated by EMG. *Clin. Neurophysiol. 118* (8), 1877−1888.
(23) Castro, S., Falconi, A., Chase, M. H., and Torterolo, P. (2013) Coherent Neocortical 40-Hz Oscillations Are Not Present during REM Sleep. *Eur. J. Neurosci. 37* (8), 1330−1339.
(24) Cavelli, M., Castro, S., Schwarzkopf, N., Chase, M. H., Falconi, A., and Torterolo, P. (2015) Coherent Neocortical Gamma Oscillations Decrease during REM Sleep in the Rat. *Behav. Brain Res. 281*, 318−325.
(25) Cavelli, M., Castro-Zaballa, S., Mondino, A., Gonzalez, J., Falconi, A., and Torterolo, P. (2017) Absence of EEG Gamma Coherence in a Local Activated Cortical State: A Conserved Trait of REM Sleep. *Transl. Brain Rhythm. 2*, No. 115, DOI: 10.15761/TBR.1000115.
(26) González, J., Cavelli, M., Mondino, A., Pascovich, C., Castro-Zaballa, S., Torterolo, P., and Rubido, N. (2019) Decreased Electrocortical Temporal Complexity Distinguishes Sleep from Wakefulness. *Sci. Rep. 9* (1), 18457.
(27) Bandt, C., and Pompe, B. (2002) Permutation Entropy: A Natural Complexity Measure for Time Series. *Phys. Rev. Lett. 88* (17), 174102.
(28) Carhart-Harris, R. L., Leech, R., Hellyer, P. J., Shanahan, M., Feilding, A., Tagliazucchi, E., Chialvo, D. R., and Nutt, D. (2014) The Entropic Brain: A Theory of Conscious States Informed by Neuroimaging Research with Psychedelic Drugs. *Front. Hum. Neurosci. 8*, 20.
(29) Carhart-Harris, R. L., Muthukumaraswamy, S., Roseman, L., Kaelen, M., Droog, W., Murphy, K., Tagliazucchi, E., Schenberg, E. E., Nest, T., Orban, C., Leech, R., Williams, L. T., Williams, T. M., Bolstridge, M., Sessa, B., McGonigle, J., Sereno, M. I., Nichols, D., Hellyer, P. J., Hobden, P., Evans, J., Singh, K. D., Wise, R. G., Curran, H. V., Feilding, A., and Nutt, D. J. (2016) Neural Correlates of the LSD Experience Revealed by Multimodal Neuroimaging. *Proc. Natl. Acad. Sci. U. S. A. 113* (17), 4853−4858.
(30) Pallavicini, C., Vilas, M. G., Villarreal, M., Zamberlan, F., Muthukumaraswamy, S., Nutt, D., Carhart-Harris, R., and Tagliazucchi, E. (2019) Spectral Signatures of Serotonergic Psychedelics and Glutamatergic Dissociatives. *NeuroImage 200*, 281−291.
(31) Timmermann, C., Roseman, L., Schartner, M., Milliere, R., Williams, L. T. J., Erritzoe, D., Muthukumaraswamy, S., Ashton, M., Bendrioua, A., Kaur, O., Turton, S., Nour, M. M., Day, C. M., Leech, R., Nutt, D. J., and Carhart-Harris, R. L. (2019) Neural Correlates of the DMT Experience Assessed with Multivariate EEG. *Sci. Rep. 9* (1), 16324.
(32) Pallavicini, C., Cavanna, F., Zamberlan, F., de la Fuente, L. A., Perl, Y. S., Arias, M., Romero, C., Carhart-Harris, R., Timmermann, C., and Tagliazucchi, E. (2020) Neural and Subjective Effects of Inhaled DMT in Natural Settings, v 1, *bioRxiv*, DOI: 10.1101/2020.08.19.258145.

(33) Lockmann, A. L. V., Laplagne, D. A., Leão, R. N., and Tort, A. B. L. (2016) A Respiration-Coupled Rhythm in the Rat Hippocampus Independent of Theta and Slow Oscillations. *J. Neurosci. 36* (19), 5338−5352.
(34) Tort, A. B. L., Brankačk, J., and Draguhn, A. (2018) Respiration-Entrained Brain Rhythms Are Global but Often Overlooked. *Trends Neurosci. 41* (4), 186−197.
(35) Sanz, C., Zamberlan, F., Erowid, E., Erowid, F., and Tagliazucchi, E. (2018) The Experience Elicited by Hallucinogens Presents the Highest Similarity to Dreaming within a Large Database of Psychoactive Substance Reports. *Front. Neurosci. 12*, 7.
(36) Siclari, F., Baird, B., Perogamvros, L., Bernardi, G., LaRocque, J. J., Riedner, B., Boly, M., Postle, B. R., and Tononi, G. (2017) The Neural Correlates of Dreaming. *Nat. Neurosci. 20* (6), 872−878.
(37) Glick, S. D., Maisonneuve, I. M., Hough, L. B., Kuehne, M. E., and Bandarage, U. K. (2006) (±)-18-Methoxycoronaridine: A Novel Iboga Alkaloid Congener Having Potential Anti-Addictive Efficac. *CNS Drug Rev. 5*, 27 DOI: 10.1111/j.1527-3458.1999.tb00084.x.
(38) Helsley, S., Fiorella, D., Rabin, R. A., and Winter, J. C. (1998) Behavioral and Biochemical Evidence for a Nonessential 5-HT2A Component of the Ibogaine-Induced Discriminative Stimulus. *Pharmacol., Biochem. Behav. 59* (2), 419−425.
(39) Helsley, S., Rabin, R. A., and Winter, J. C. (1997) The Effects of Noribogaine and Harmaline in Rats Trained with Ibogaine as a Discriminative Stimulus. *Life Sci. 60* (9), PL147−153.
(40) Mash, D. C., Staley, J. K., Baumann, M. H., Rothman, R. B., and Hearn, W. L. (1995) Identification of a Primary Metabolite of Ibogaine That Targets Serotonin Transporters and Elevates Serotonin. *Life Sci. 57* (3), PL45−50.
(41) Baumann, M. H., Rothman, R. B., Pablo, J. P., and Mash, D. C. (2001) In Vivo Neurobiological Effects of Ibogaine and Its O-Desmethyl Metabolite, 12-Hydroxyibogamine (Noribogaine), in Rats. *J. Pharmacol. Exp. Ther. 297* (2), 531−539.
(42) Rodríguez, P., Urbanavicius, J., Prieto, J. P., Fabius, S., Reyes, A. L., Havel, V., Sames, D., Scorza, C., and Carrera, I. (2020) A Single Administration of the Atypical Psychedelic Ibogaine or Its Metabolite Noribogaine Induces an Antidepressant-like Effect in Rats. *ACS Chem. Neurosci. 11*, 1661.
(43) Chen, K., Kokate, T. G., Donevan, S. D., Carroll, F. I., and Rogawski, M. A. (1996) Ibogaine Block of the NMDA Receptor: In Vitro and in Vivo Studies. *Neuropharmacology 35* (4), 423−431.
(44) Layer, R. T., Skolnick, P., Bertha, C. M., Bandarage, U. K., Kuehne, M. E., and Popik, P. (1996) Structurally Modified Ibogaine Analogs Exhibit Differing Affinities for NMDA Receptors. *Eur. J. Pharmacol. 309* (2), 159−165.
(45) Mash, D. C., Staley, J. K., Pablo, J. P., Holohean, A. M., Hackman, J. C., and Davidoff, R. A. (1995) Properties of Ibogaine and Its Principal Metabolite (12-Hydroxyibogamine) at the MK-801 Binding Site of the NMDA Receptor Complex. *Neurosci. Lett. 192* (1), 53−56.
(46) Popik, P., Layer, R. T., and Skolnick, P. (1994) The Putative Anti-Addictive Drug Ibogaine Is a Competitive Inhibitor of [3H]MK-801 Binding to the NMDA Receptor Complex. *Psychopharmacology (Berl.) 114* (4), 672−674.
(47) Popik, P., Layer, R. T., Fossom, L. H., Benveniste, M., Geter-Douglass, B., Witkin, J. M., and Skolnick, P. (1995) NMDA Antagonist Properties of the Putative Antiaddictive Drug, Ibogaine. *J. Pharmacol. Exp. Ther. 275* (2), 753−760.
(48) Staley, J. K., Ouyang, Q., Pablo, J., Hearn, W. L., Flynn, D. D., Rothman, R. B., Rice, K. C., and Mash, D. C. (1996) Pharmacological Screen for Activities of 12-Hydroxyibogamine: A Primary Metabolite of the Indole Alkaloid Ibogaine. *Psychopharmacology (Berl.) 127* (1), 10−18.
(49) Ahnaou, A., Huysmans, H., Biermans, R., Manyakov, N. V., and Drinkenburg, W. H. I. M. (2017) Ketamine: Differential Neurophysiological Dynamics in Functional Networks in the Rat Brain. *Transl. Psychiatry 7* (9), No. e1237.
(50) Caixeta, F. V., Cornélio, A. M., Scheffer-Teixeira, R., Ribeiro, S., and Tort, A. B. L. (2013) Ketamine Alters Oscillatory Coupling in the Hippocampus. *Sci. Rep. 3*, 2348.
(51) Castro-Zaballa, S., Cavelli, M. L., Gonzalez, J., Nardi, A. E., Machado, S., Scorza, C., and Torterolo, P. (2019) EEG 40 Hz Coherence Decreases in REM Sleep and Ketamine Model of Psychosis. *Front. Psychiatry 9*, 766.
(52) Manduca, J. D., Thériault, R.-K., Williams, O. O. F., Rasmussen, D. J., and Perreault, M. L. (2020) Transient Dose-Dependent Effects of Ketamine on Neural Oscillatory Activity in Wistar-Kyoto Rats. *Neuroscience 441*, 161.
(53) Coleman, J. A., Yang, D., Zhao, Z., Wen, P.-C., Yoshioka, C., Tajkhorshid, E., and Gouaux, E. (2019) Serotonin Transporter-Ibogaine Complexes Illuminate Mechanisms of Inhibition and Transport. *Nature 569* (7754), 141−145.
(54) Jacobs, M. T., Zhang, Y.-W., Campbell, S. D., and Rudnick, G. (2007) Ibogaine, a Noncompetitive Inhibitor of Serotonin Transport, Acts by Stabilizing the Cytoplasm-Facing State of the Transporter. *J. Biol. Chem. 282* (40), 29441−29447.
(55) Maillet, E. L., Milon, N., Heghinian, M. D., Fishback, J., Schürer, S. C., Garamszegi, N., and Mash, D. C. (2015) Noribogaine Is a G-Protein Biased κ-Opioid Receptor Agonist. *Neuropharmacology 99*, 675−688.
(56) Young, G. A., and Khazan, N. (1984) Differential Neuropharmacological Effects of Mu, Kappa and Sigma Opioid Agonists on Cortical EEG Power Spectra in the Rat. Stereospecificity and Naloxone Antagonism. *Neuropharmacology 23* (10), 1161−1165.
(57) Coltro Campi, C., and Clarke, G. D. (1995) Effects of Highly Selective Kappa-Opioid Agonists on EEG Power Spectra and Behavioural Correlates in Conscious Rats. *Pharmacol., Biochem. Behav. 51* (4), 611−616.
(58) Tortella, F. C., Rose, J., Robles, L., Moreton, J. E., Hughes, J., and Hunter, J. C. (1997) EEG Spectral Analysis of the Neuroprotective Kappa Opioids Enadoline and PD117302. *J. Pharmacol. Exp. Ther. 282* (1), 286−293.
(59) Bokil, H., Andrews, P., Kulkarni, J. E., Mehta, S., and Mitra, P. P. (2010) Chronux: A Platform for Analyzing Neural Signals. *J. Neurosci. Methods 192* (1), 146−151.
(60) Tort, A. B. L., Komorowski, R., Eichenbaum, H., and Kopell, N. (2010) Measuring Phase-Amplitude Coupling Between Neuronal Oscillations of Different Frequencies. *J. Neurophysiol. 104* (2), 1195−1210.
(61) Delorme, A., and Makeig, S. (2004) EEGLAB: An Open Source Toolbox for Analysis of Single-Trial EEG Dynamics Including Independent Component Analysis. *J. Neurosci. Methods 134* (1), 9−21.